THE JOURNAL OF
PHYSICAL CHEMISTRY C

Article

pubs.acs.org/JPCC

Strong and Long-Lived Free-Radical Oxidizer Based on Silver(II). Mechanism of Ag(I) Electrooxidation in Concentrated H_2SO_4

Piotr Połczyński,[†] Rafal Jurczakowski,[†,*] and Wojciech Grochala[†,‡]

[†]Faculty of Chemistry, University of Warsaw, Pasteur 1, PL-02-093 Warsaw, Poland

[‡]Center for New Technologies, University of Warsaw, Żwirki i Wigury 93, PL-02-089 Warsaw, Poland

Ⓢ *Supporting Information*

ABSTRACT: Electrooxidation of silver(I) was studied in concentrated sulfuric acid and oleums at fluorine-doped tin oxide electrode. Electrochemical processes taking place at the electrode/solution interface have been investigated by using classical transient methods. We report a catalytic reaction pathway, in which one-electron transfer leading to solvated Ag(II) species is followed by a homogeneous chemical step with regeneration of depolarizer. By means of digital simulations this mechanism and the half-life of the Ag(II) complex was determined, $\tau_{1/2}$ = 10 s. Activation energies of the electrode process and chemical reaction were found to be $E_{a,E}$ = 52 ± 5 kJ·mol^{-1} and $E_{a,C}$ = 60 ± 5 kJ·mol^{-1}, respectively. The chemical step likely corresponds to a free-radical oxidation of HSO_4^- anions by Ag(II) radical species. Highly oxidative abilities of long-lived Ag(II) can be used for mediated electrochemical oxidation or electrochemical combustion.

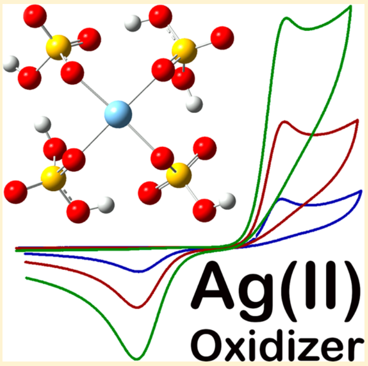

1. INTRODUCTION

Silver(II) is a powerful one-electron oxidizer with the standard redox potential, E^0, for the Ag(II)/Ag(I) redox couple reaching nearly +2 V,[1,2] thus exceeding those for nearly all organic redox couples. This renders Ag(II) as a useful electron-transfer reagent since electrochemically generated divalent silver can be used as an extinction agent for oxidation of organic chemical pollutions in wastewater[3,4] or as an bactericide.[5] Ag(II) also readily attacks many inorganic species[6] and has been utilized for treatment of nuclear waste,[7] extinction of ozone-depleting freons,[8] and of selected greenhouse gases.[9] Silver(I) used for efficient MEO (mediated electrochemical oxidation) may be recovered from postelectrolysis solutions.[10]

Because of high standard potential of the Ag(II)/Ag(I) redox couple divalent silver compounds have a rather short lifetime in solutions containing unbounded water.[11] Moreover, solvent, electrolyte, and electrode material itself has to be highly resistant to oxidation to permit studies of Ag(II) electrogeneration. From Pourbaix diagram, it follows that Ag(II) can be only produced in solutions more acidic than pH = −2[12] since in less acidic or neutral solutions the mixed-valence $Ag_7O_8^+$ clathrate salts are electrocrystallized.[13] To date, electrochemical oxidation of Ag(I) was studied mostly at platinum electrodes in aqueous solutions of nitric, perchloric, and sulfuric acids of moderate concentrations[6,8,14] with just one report using 95% H_2SO_4.[15] However, platinum is not appropriate electrode material in studies involving highly anodic potentials in excess of +1.5 V versus RHE in the concentrated sulfuric acid environment since electrode material undergoes chemical deterioration (etching) at these conditions.[16,17] To overcome these problems, materials such as glassy carbon, Pt grown on Ti substrate, β-PbO_2, and TiO_{2-x} ceramic anodes were investigated to find a substitute for Pt.[18] However, the rate of oxidation of Ag(I) was about 4 times lower for these materials than for pure Pt electrode. Two other studies have utilized a boron-doped diamond (BDD) electrodes for electrooxidation of silver(I).[19,20] The BDD electrodes have a broad potential window in aqueous solutions, exhibit low adsorption properties, kinetics of Ag(I) electrooxidation comparable to that for 5 μm Pt-covered Ti electrodes, and they are chemically inert in aggressive chemical media.

In our recent preliminary report, we have studied the electrooxidation of silver(I) in concentrated sulfuric acid solutions and oleums at fluorine-doped tin oxide electrodes (FTO).[21] Unlike platinum, FTO electrode is chemically inert at anodic potentials and harsh acidic chemical environment;[22] it is also inexpensive as compared to the BDD electrodes. We have observed that the formal redox potential, $E^{\circ\prime}$, of the Ag(II)/Ag(I) redox pair is markedly dependent on the Hammett acidity function, H_0, in particular for superacidic region of $H_0 < -13$. $E^{\circ\prime}$ reaches the value of +2.90 V versus NHE in 33% oleum ($H_0 = -14$) thus exceeding the standard redox potential, E^0, of the ($OH^\bullet$,H^+/H_2O) redox couple (+2.73 V),[23,24] of the related ($SO_4^{\bullet-}$/SO_4^{2-}) couple (+2.43 V to +2.60 V),[23,25] while rivaling E^0 for the (F_2/$2F^-$) one (+2.87 V).[1] This means that at highly anodic potentials exceeding +2.8 V versus NHE electrooxidation of silver(I) may compete with the oxidation of solvent (unbound water,[14,19] HSO_4^- or related anions,[26] or even of neutral sulfuric acid). The purpose of the current contribution is to extend the preliminary study[21] by elucidating

Received: June 29, 2013
Revised: August 29, 2013
Published: September 4, 2013

the mechanism of the electrochemical processes taking place at the electrode/solution interface at various concentrations of sulfuric acid and oleums.

2. EXPERIMENTAL SECTION

Materials. Silver(I) sulfate (Sigma Aldrich, 99.999%) and 65% oleum (Sigma Aldrich, 99.99%) were used without further purification. Ninety-five percent sulfuric acid (99.99%, POCh) was twice distilled in subboiling quartz still to eliminate impurities, which otherwise influenced results to a large extent.

The solutions of <95% H_2SO_4 were prepared from 95% H_2SO_4 and triply distilled water additionally purified by Millipore filters (18.2 MΩ cm^2). Higher acid concentrations and oleums of a given concentration were prepared from 95% H_2SO_4 and 20% oleum (for the target H_2SO_4 concentration of up to 125%) and from 95% H_2SO_4 and 65% oleum (for higher target concentrations). The achieved concentrations of the acid and oleums were determined by conductometric titration of H_2SO_4 by 65% oleum. The precise concentration can be determined by using this procedure since conductivity of the acid is strongly dependent on its concentration with minimum of conductance at 100% H_2SO_4.[27] Obtained values were additionally confirmed by density measurements. The largest concentration of oleum used was 33% (corresponding to 140% H_2SO_4), as for higher oleum concentrations (40−65%, i.e., concentrations of H_2SO_4 up to 180%) the position of the small anodic signal (which is overlapped with large O_2 evolution wave) could not be determined precisely.

All glassware was thoroughly cleaned prior to use with "piranha solution" (1:10 per volume of 30% H_2O_2 and 95% H_2SO_4, respectively) at 80 °C.

Electrochemical Measurements. Electrochemical measurements were performed using the classical transient methods. The three-electrode setup in thermostatted electrochemical glass cell with two separated compartments was applied. Cell was hermetic with inert gas constant flow through solution or above it. N6.7 Ar gas with pressure regulator and gas lines of corresponding purity were used for deareation of electrolyte solution. All joints for argon inlet and outlet were made of Teflon. Commercially available FTO electrodes 2.2 mm thick sodalime glass coated on one side with a fluorine-doped tin oxide (SnO_2:F) layer were used as working electrodes. The sheet resistance of the FTO layer was ~7 Ω/sq. (SOLARONIX SA, Switzerland). FTO electrodes were embedded in Teflon and surface area exposed to the solution was $A = 0.04$ cm^2. To improve the reproducibility of the results the FTO electrodes were electrochemically cleaned by potential cycling in pure acid. Platinum sheet of large surface area >10 cm^2 was used as counter electrode. The reference electrode selection is also demanding since classical electrodes with aqueous electrolytes have to be excluded from obvious reasons. Here, the electrode potentials was measured versus saturated silver(I) sulfate electrode (SSE) in concentrated sulfuric acid $Ag/Ag_2SO_{4(sat)}/H_2SO_4$ (95%) that was separated from the working electrode compartment by a glass tube bridge filled with the tested solution. The potential of the SSE electrode versus normal hydrogen electrode (NHE) cannot be measured directly and can be only estimated. Moreover, the respective measurement of SSE potential versus reversible hydrogen electrode (RHE) also cannot be performed directly because of the platinum dissolution in sulphuric acid at concentrations >14 M.[16] The estimation of the reference electrode potential versus NHE and the procedure aiming to elimination of the liquid junction potential (LJP) was discussed in our previous contribution.[21] In this work, all potentials are given versus the SSE electrode. The potential of this electrode was estimated to be +0.8 V versus NHE.

Electrochemical measurements were performed by using Solartron-Shlumberger 1287A potentiostat controlled by CorrWare from Scribner Associates. All measurements were carried out at 25 °C with temperature control provided by thermostat.

The ESR spectra were recorded using a CW X-band BrukerELEXYS 500 system equipped with the liquid nitrogen heating−cooling setup. The measurements were performed at 125, 135, 200, 250, 270, and 300 K for solution after electrolysis and obtained precipitate. The OR−C cavity was mounted to the spectrometer.

3. RESULTS AND DISCUSSION

3.1. Current−Potential Characteristics of Ag(I) Electroxidation.

Cyclic voltamperomeric curves registered at FTO in pure sulphuric acid (in 95% H_2SO_4) and in the presence of Ag_2SO_4 at different concentrations is presented in Figure 1 (top). In pure acid, within the potential range from +0.5 to +2.5 V, only double layer charging current is observed. At higher potentials, a halfwave related to oxygen evolution is seen (its onset is shown here). Oxygen production is a two-step reaction proceeding via electrogeneration of peroxydisulfuric acid (or its anions) and their further decomposition with evolution of elemental oxygen (eqs 1, 2)

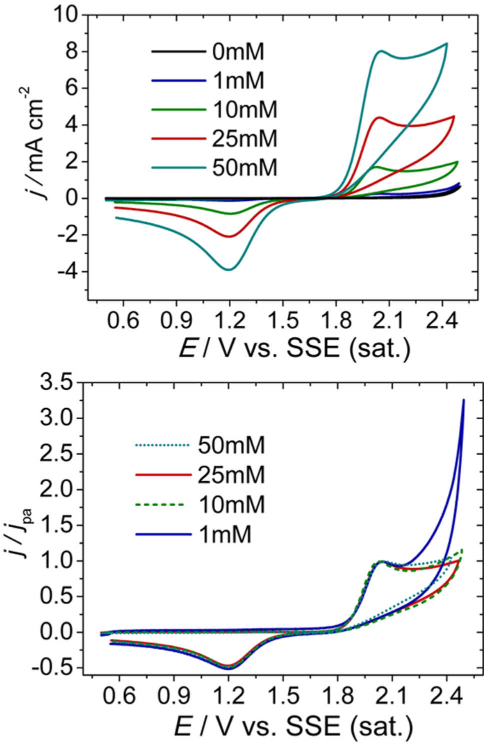

Figure 1. Top: Cyclic voltammograms registered at FTO electrode in 95% H_2SO_4 for different silver(I) concentrations ($c_{Ag(I)}$ 0; 1.0; 10, 25, and 50 mM), scan rate ν = 500 mV·s^{-1}. Bottom: The same curves normalized to anodic current peak ($j_{p,a}$ = 0.55, 1.7, 4.4, and 8 mA cm^{-2} for 1, 10, 25, and 50 mM, respectively).

$$2HSO_4^- \rightarrow S_2O_8^{2-} + 2e^- + 2H^+ \quad E^0 = +2.08V \tag{1}$$

The reaction described by eq 1 is catalyzed in the presence of cations of metal such as silver, copper, and iron, which act as electron carriers.[1]

In the concentrated sulfuric acid or in oleums that are free of chemically unbound water,[28] the following reaction can be expected

$$2HS_2O_8^- \rightarrow 2HS_2O_7^- + O_2\uparrow \qquad (2)$$

In cathodic scan, the oxidations product is reduced at potential below +1.6 V. Cyclic voltammograms registered for different concentrations of Ag_2SO_4 in 95% H_2SO_4 at scan rate 500 mV/s have revealed that anodic peak current in function of depolarizer concentration (Ag(I)) satisfies the Randles-Sevcik equation with 99% goodness. The apparent diffusion coefficient of Ag(I) ions determined from this dependence is equal to $D_{red} = 4.2 \times 10^{-7}$ $cm^2 \cdot s^{-1}$.[29] This clearly suggests that it is Ag(I) that undergoes electrooxidation. Figure 1 (bottom) shows that when currents are normalized to anodic peak all curves largely overlap within a wide potential range 0.6−2.1 V (Figure 1, bottom). It should be stressed that this is an important observation from the mechanistic point of view as will be discussed later.

The influence of scan rates on cyclic voltammogram characteristics is shown in Figure 2. Separation between anodic and cathodic peaks is within the range 500−1000 mV for scan rate ranging from 10 to 1000 mV/s, respectively; this indicates that the electrode reaction is quasi-reversible. A similar voltammetric behavior was reported for electrooxidation of Ag^+ in 4 M HNO_3 on BDD electrodes.[20] The dependence of the formal potential, $E°'$, on acidity of the solvent, as measured by the Hammett acidity function, H_0,[30] was discussed in our previous report.[21] It should be noticed that not only the peaks separation, but also the cathodic to anodic peak current ratio, i_c/i_a, is strongly affected by the scan rate. The i_c/i_a ratio is related to concentration distribution of oxidized and reduced species near the electrode surface.

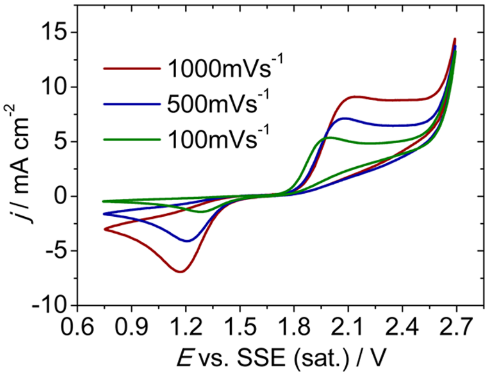

Figure 2. (A) Cyclic voltammograms registered in 95% H_2SO_4 containing 75 mM Ag(I) at FTO electrode with different scan rates, *v*.

The quotient of anodic to cathodic current peaks in function of time, *t*, elapsed between both peaks is shown in Figure 3. This relationship was fitted with an exponential function (eq 3) with 99% goodness

$$C(t) = C_1 + C_0 2^{-t/\tau_{1/2}} \qquad (3)$$

This result suggests that the electrochemical step is followed by a (pseudo)first order homogeneous reaction leading to concentration decrease of the oxidized form. The apparent half-life of the oxidized form is 5 s that corresponds to value rate constant of homogeneous reaction of 0.14 s^{-1}. However, it should be noted that this value is only an estimation since the cathodic to anodic peak ratio for EC mechanism is described by more complex function of time.[29] First order kinetics is not an unexpected result since previous electrochemical and spectrophotometric studies have revealed that the electrogenerated Ag(II) species slowly oxidize solvent via a (pseudo)first order reaction.[11] Also the 4−18 M H_2SO_4 readily undergoes oxidation with Ag(II).[15] However, second order kinetics was also observed in spectrophotometric studies in nitric acid (see ref 31 and references therein) and in 3 M $HClO_4$.[22] Second order kinetics implies disproportionation of silver(II) to +1 and +3 oxidation state. The latter process is less pronounced at higher acid concentrations[22] and is therefore less probable in our system. Indeed, anodic to cathodic current peak ratio is not dependent on silver(I) concentration as evidenced in bottom part of Figure 1. This result confirms (pseudo)first order chemical step and lack of disproportionation stage in the reaction mechanism.

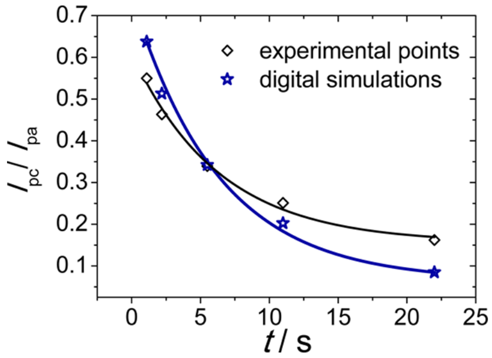

Figure 3. Exponential decay of the anodic to cathodic current peaks ratio, $I_{p,c}/I_{p,a}$, registered during voltammetric measurements: (diamonds, ◇) experimental data, (stars, ★) digital simulations.

3.2. The Additional Anodic Peak. When the electrode potential is scanned toward more positive potentials the additional broad anodic peak appears in the cyclic voltammograms at potential *circa* 300 mV higher than that of the main electrode process (Figure 2). It does not have its cathodic counterpart in the potential range measured. For voltammogram registered for 1 mM Ag(I) and shown Figure 1 (bottom), the rapid current growth at potential $E > 2.1$ V is related to pure acid oxidation since the same current is observed in the absence of silver(I) in the solution. Hence, given substantial acidity of the environment, this process is most likely related generation of hydrogensulphate free radical, $HSO_4^\bullet$

$$H_2SO_4 \rightarrow HSO_4^\bullet + e^- + H^+ \qquad (4)$$

The free radical species can be also catalytically electrogenerated by oxidation of HSO_4^- anions in the presence of Ag(I) catalyst,[1] which may be the origin of the additional faradaic currents at potentials exceeding +2.3 V versus SSE in the CVs at higher silver concentrations.[32]

3.3. The Numerical Model of Electrode and Chemical Reactions. Further insight into the mechanism and kinetics of electrode reaction was achieved by means of digital simulation of the electrode process. The main electrode reaction is described by eq 6. The catalytic reaction, in which depolarizer is reproduced in the chemical step, is described by eq 7. This core model was additionally fine-tuned by introduction of reactions

8 and 9. Reaction 8 describes additional electrode process catalyzed by the presence of Ag^+ leading to reactive species (presumably free radical moieties such as $HSO_4^{\bullet}$ radicals). Finally reaction described by eq 5 is responsible, inter alia, for oxygen evolution since

$$4HSO_4^{\bullet} \rightarrow 2H_2S_2O_8 \rightarrow 2H_2S_2O_7 + O_2\uparrow \tag{5}$$

Hence, the model can be in general described by the following reaction sequence

$$\mathrm{Red}_1 \underset{k_{-1}}{\overset{k_1}{\rightleftarrows}} \mathrm{Ox}_1 + e^- \tag{6}$$

$$\mathrm{Ox}_1 + \mathrm{A} \xrightarrow{k_2} \mathrm{Red}_1 + \mathrm{B} \tag{7}$$

$$\mathrm{Red}_2 \underset{k_{-3}}{\overset{k_3}{\rightleftarrows}} \mathrm{Ox}_2 + e^- \tag{8}$$

$$2\mathrm{Ox}_2 \xrightarrow{k_4} \mathrm{C} \tag{9}$$

When compound A is present in a large excess, one may simplify the chemical step to a pseudo-first order reaction $\mathrm{Ox} + \mathrm{A} \xrightarrow{k} \mathrm{Red}$, in which the homogeneous rate constant $k = k_2[\mathrm{A}]$. Faradaic dc current, i_f, related to reactions 6−9, is

$$i_f = FA \sum_j n_j[k_{b,j}C_{\mathrm{red},j}(0, t) - k_{f,j}C_{\mathrm{ox},j}(0, t)] \tag{10}$$

where $j = 1$ and 2; n is the number of electrons exchanged in the electrode processes, $C_{\mathrm{ox},j}(0,t)$ and $C_{\mathrm{red},j}(0,t)$ are the surface concentrations of the Ox_j and Red_j species, respectively. $k_{f,j}$ and $k_{b,j}$ are the heterogeneous rate constants of the forward (reduction) and backward (oxidation) processes:

$$k_{f,j} = k_{0,j} \exp[-\propto_j nf(E - E_j^{0'})] \tag{11}$$

$$k_{b,j} = k_{0,j} \exp[\beta_j nf(E - E_j^{0'})] \tag{12}$$

where $E_j^{0\prime}$ is the formal potential, $f = F/RT$, $n = 1$ and other symbols have their usual meaning. Assuming a simplified model of linear diffusion in the semi-inifinite space along direction x (normal to the electrode surface), the concentrations of species Ox_j and Red_j are described by Fick's law, in which chemical step was included

$$\frac{\partial C_{\mathrm{ox},1}}{\partial t} = D_{\mathrm{ox},1}\frac{\partial^2 C_{\mathrm{ox},1}}{\partial x^2} - k_2 C_{\mathrm{ox},1} \tag{13}$$

$$\frac{\partial C_{\mathrm{red},1}}{\partial t} = D_{\mathrm{red},1}\frac{\partial^2 C_{\mathrm{red},1}}{\partial x^2} + k_2 C_{\mathrm{ox},1} \tag{14}$$

$$\frac{\partial C_{\mathrm{red},2}}{\partial t} = D_{\mathrm{ox},2}\frac{\partial^2 C_{\mathrm{red},2}}{\partial x^2} \tag{15}$$

$$\frac{\partial C_{\mathrm{ox},2}}{\partial t} = D_{\mathrm{red},2}\frac{\partial^2 C_{\mathrm{ox},2}}{\partial x^2} - 2k_4 C_{\mathrm{ox},2}^2 \tag{16}$$

By using finite difference method, eqs 13−16 were numerically solved with the following boundary and initial conditions

$$\begin{aligned} &t < 0 \quad E = E_1,\ C_{\mathrm{red},1} = C_{\mathrm{red},1}^*,\ C_{\mathrm{red},2} = C_{\mathrm{red},2}^*,\ C_{\mathrm{Ox},1} = C_{\mathrm{Ox},2} = 0 \\ &t > 0 \qquad\qquad E = E_1 + vt \end{aligned} \tag{17}$$

$$\begin{aligned} &t > 0,\ x \rightarrow \infty \\ &C_{\mathrm{red},1} = C_{\mathrm{red},1}^*,\ C_{\mathrm{red},2} = C_{\mathrm{red},2}^*,\ C_{\mathrm{Ox},1} = C_{\mathrm{Ox},2} = 0 \end{aligned} \tag{18}$$

The parameters for reactions 6−9 were obtained in the following way. First, the transfer coefficient β_1 was determined from logarithmic analysis of the deconvoluted voltammetric anodic runs. This parameter influences both peaks separation on the potential scale and ratio of cathodic to anodic current peaks and therefore has to be determined before heterogeneous and homogeneous rate constants are established. For reaction 8, the free radical $HSO_4^{\bullet}$ radical formation was assumed and the standard potential of $SO_4^{\bullet-}/SO_4^{2-}$ independent of pH, $E^0 = +2{,}6$ V versus NHE, was taken from literature.[26] Chemical recombination of $SO_4^{\bullet-}$ radicals rate constant, $k_4 = 3.8 \times 10^8$ $\mathrm{dm^3\ mol^{-1}\ s^{-1}}$, was taken from literature.[42] Other parameters were found by comparison between experimental and simulated cyclic voltammetric curves. Results for 75 mM of Ag(I) in concentrated H_2SO_4 at scan rate 500 mV/s in potential range 0.5−3.0 V versus SSE for two different temperatures 263 and 298 K are shown in Figure 6. The heterogeneous rate constant for reaction 6 was found to be $k_{s,1} = 2 \times 10^{-6}$ $\mathrm{cm{\cdot}s^{-1}}$ and for the homogeneous chemical step (7) $k_2 = 0.07$ $\mathrm{s^{-1}}$, which corresponds to half-life $\tau_{1/2} = 10$ s. The agreement between the measured and simulated CV curves confirms the correctness of the proposed model. From simulation in different temperatures, activation energies were determined while applying the Arrhenius equation (Figure 7). Activation energies of the electrode process and chemical reaction were found to be $E_{a,E} = 52 \pm 5$ $\mathrm{kJ{\cdot}mol^{-1}}$ and $E_{a,C} = 60 \pm 5$ $\mathrm{kJ{\cdot}mol^{-1}}$, respectively. The fact that the latter value is larger than the former comes in part from a stronger and more covalent binding of anions and solvent to the Ag(II) cation (substrate of the chemical reaction) than to the Ag(I) one (substrate of the electrochemical reaction).

3.4. The Influence of the Solution Acidity on the Formal Potential.

The influence of sulphuric acid concentrations on voltammetric characteristics was discussed in detail in the preceding report[21] but we will remind it here briefly for consistency of this study. We have observed that the formal redox potential for the Ag(II)/Ag(I) couple is strongly dependent on H_0 and it reaches the value close to +2 V versus SSE for 33% oleum that corresponds to +2.9 V versus NHE.[21] The slope of the $E^{\circ\prime}$ versus H_0 relationship takes two different values depending on the acidity range, which correspond to a proton to electron ratio of ca. 1.33 (for $H_0 > -13$) and 3.0 (for $H_0 < -13$). Thus, the $E^{\circ\prime}$ versus H_0 dependence bends in the vicinity of H_0 value of H_2SO_4, which suggests that electrode processes are connected to acid−base equilibria typical of concentrated H_2SO_4 and oleums.

Considering these dissociation equilibria,[28] the electrode processes may be approximated by the following reaction equations in which proton to electron ratio $H^+/e^- = 4/3$ is taken into account (eqs 19−20)[21]

$$3Ag^+ + 4H_2SO_4 + 2HSO_4^- \rightarrow 3Ag(HSO_4)_{2(\mathrm{solv})} + 4H^+ + 3e^- \quad (\text{for } H_0 > -13) \tag{19}$$

$$Ag^+ + H_2SO_4 + H_3SO_4^+ \rightarrow Ag(HSO_4)_{2(\mathrm{solv})} + 3H^+ + e^- \quad (\text{for } H_0 < -13) \tag{20}$$

Of course, these reactions equations should be treated as tentative since similar ratios may be achieved for other chemical formulas and proportions of reactants and products. The chemical nature of the oxidized Ag(II) product is discussed in the next section.

3.5. The Nature of the Ag(II) Species in Solution. Two types of Ag(II) complexes in 4−18 M H_2SO_4 (characterized by different absorption maxima in the NUV region) have been detected in the previous studies, but chemical identity of these complexes has not been established.[15] It is quite possible that they contain ligated water molecules, which renders them irrelevant to the conditions typical of the 100% H_2SO_4 and oleums (see ESI). Here we have tentatively assumed that solvated $Ag(HSO_4)_2$ constitutes the reaction product in the proposed reactions taking place at highly acidic conditions (cf. eqs 19 and 20). But in the ionizing solvent, such as nearly completely dissociated H_2SO_4, this assumption may not be true, and ionic forms such as solvated $Ag(HSO_4)^+$ or $Ag(HSO_4)_3^-$ may be anticipated. In order to get better insight into the nature of the Ag(II) species in solution, we have conducted spectroelectrochemical and ESR spectroscopic measurements for the yellow solutions obtained via electrolysis of $AgHSO_4$ in H_2SO_4 solutions at +2.5 V versus SSE.

The ESR spectrum of the postelectrolysis solution is presented in Figure 4 (for calculations cf. ESI). The spectrum is quite strong and it contains three sharp components indicating a rhombic **g** tensor, overlapped with a broader feature. The **g** values for the three sharp components are $g_1 = 2.09$, $g_2 = 2.13$, $g_3 = 2.43$ suggesting that solvated paramagnetic Ag(II) is found in the distorted octahedral (2 + 2 + 2) ligand environment. The **g** values are typical of the close-to-tetragonal elongation of the $[AgO_6]$ octahedron with $\mathbf{g}' = (g_1 + g_2)/2 = 2.11$ and $\mathbf{g}'' = g_3 = 2.43$, and they may be compared to those measured for the tetragonally elongated Ag(II) centers in the NaF host lattice ($\mathbf{g}' = 2.10$, $\mathbf{g}'' = 2.52$[33]) consistent with the quasi-tetragonal $[AgO_4]$ coordination sphere in the theoretical model $(Ag(HSO_4)_2(H_2SO_4)_2$ in the gas phase, cf. ESI). The broad feature in the ESR spectrum is attributed to a small amount of a slowly forming dark brown solid residue, which from precipitates from the yellow solution (see Figure 4). Indeed, the separately measured ESR spectrum of the residue alone (not showed) is predominated by the above-mentioned broad feature characterized by **g** = 2.23. This testifies that the brown precipitate is a previously unknown chemical compound of Ag(II) since its **g** value is different from that of 2.087 measured for $AgSO_4$,[34] which is so far the only known Ag(II) compound with sulfate anions; in addition, the ESR spectrum of the precipitate is much narrower than that of $AgSO_4$. Detailed analysis of the chemical identity of this solid, tentatively assigned here as $Ag(HSO_4)_2$, and its magnetic properties will be described in a separate communication.

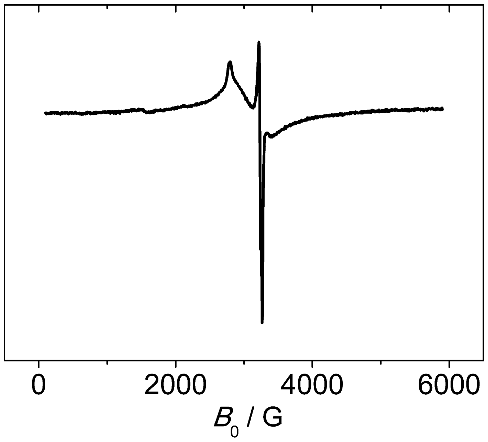

Figure 4. The ESR spectrum of the frozen yellow solution (at 125 K) obtained via a 20 h lasting electrolysis of Ag(I) in 100% H_2SO_4 (at 2.8 V vs SSE) and containing a small amount of the dark brown precipitate.

The results of the spectrophotoelectrochemistry studies of the yellow solutions are presented in Figure 5. Several bands

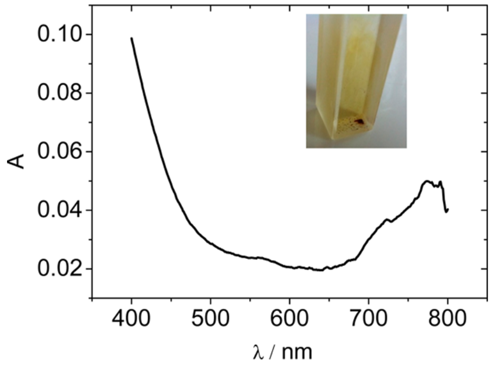

Figure 5. The vis−NIR spectra of the yellow solution obtained via a 2 h lasting electrolysis of Ag(I) in 100% H_2SO_4 (at 2.8 V vs SSE).

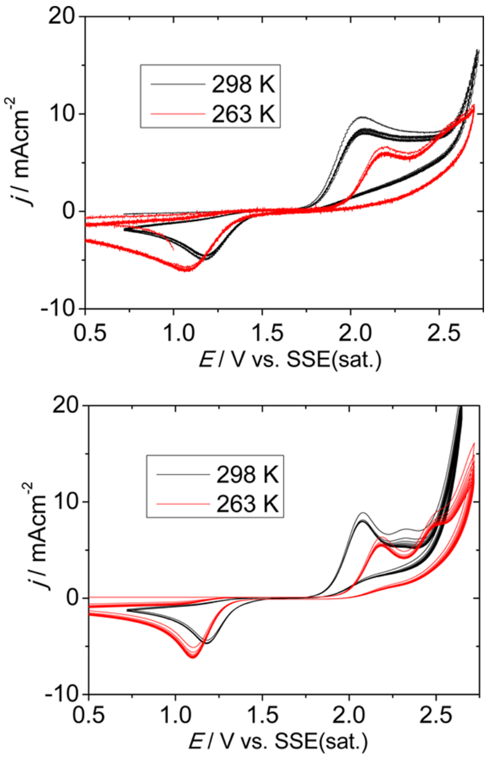

Figure 6. Comparison of experimental and simulated voltammetric profiles for two different temperatures, 298 and 263 K. (Top) Experimental CV registered at FTO electrode, scan rate $\nu = 500$ mV s^{-1} in 18 M (95%) H_2SO_4, [Ag(I)] = 75 mM. (Bottom) Digital simulations obtained for the same experimental conditions ($C_{red1} = 75$ mM) and the following parameters: $C_{red2} = 5$ M, $k_4 = 3.8 \times 10^8$ $dm^3 \cdot mol^{-1} \cdot s^{-1}$,[42] $\beta = 0.4$, $k_{s,1} = 2 \times 10^{-6}$ $cm \cdot s^{-1}$, $D_o = 4e^{-7}$ $cm^2 \cdot s^{-1}$, $E^{0\prime}_{Ag(II)/Ag(I)} = 1.65$ V, $k_2 = 0.07$ s^{-1}.

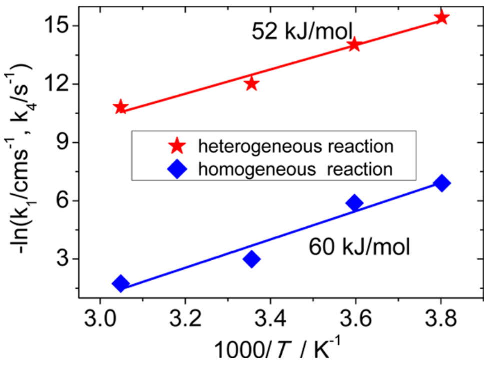

Figure 7. Arrhenius plots of the heterogeneous (blue diamonds,◆) and homogeneous (red stars,★) rate constants with activation energies calculated from the slope.

are present in the vis-NIR spectra, notably an intense tail in the violet region of the electromagnetic spectrum (i.e., 400−500 nm, responsible for the yellow color of the solutions) as well as a weak band at 570 nm (2.18 eV), a stronger shoulder maximizing at 710 nm (1.75 eV), and a part of a broad NIR band extending from 975 nm to 1100 nm (1.13−1.27 eV). As the postelectrolysis solution is kept at a room temperature, the intensity of all these bands decays in time, which is due to a spontaneous thermal decomposition of the reactive Ag(II) species and/or their reaction with solvent.

The quantum-mechanical calculations of the electronic absorption spectrum have been carried out for the $Ag(HSO_4)_2(H_2SO_4)_2$ molecules (as a model species of the Ag(II) cation solvated with two HSO_4^- anions and two neutral molecules of H_2SO_4, see Table 1 and ESI). The agreement between the measured and the theoretically predicted spectrum is fair, especially taking into account that a simplistic molecular model has been used for calculations. A weak NIR band (computed at 1041 nm) originates from the ligand-to-metal charge transfer transition O→Ag(II). A rather small energy of the charge-transfer transition is expected due to a powerfully oxidizing nature of Ag(II).

Table 1. Wavelengths of the Maxima of the Electronic Absorption Bands and the Most Intense Computed Electronic Transitions for the Isolated $Ag(HSO_4)_2(H_2SO_4)_2$ Molecules

exp. (yellow solution)	theory (td-dft)
tail 400−500 nm	424 nm
570 nm	571 nm
	651 nm
710 nm	696 nm
775 nm	801 nm
1080 nm	1041 nm

These combined experimental and theoretical results suggest that product of the electrochemical oxidation of Ag(I) in concentrated sulphuric acid could take the form of solvated $Ag(HSO_4)_2$ species.[35]

3.6. The Chemical Reaction Step. The nature of the chemical reaction step which follows the electrogeneration of Ag(II) is of interest. A substantial reactivity of $Ag(HSO_4)_{2(solv)}$ is expected based on what is known for other oxo- derivatives of divalent silver such as $AgSO_4$,[34] $Ag(SO_3F)_2$,[36] or $Ag(SO_3CF_3)_2$.[37] All these compounds are thermodynamically metastable at ambient (*p*,*T*) conditions and they decompose fast at slightly elevated temperature (~100 °C) with the formation of ligand free radicals derived from anions (such as $SO_3F^\bullet$) that may further couple to form peroxide species (i.e., $(SO_3F)_2$, and so forth). For $AgSO_4$, the thermal decomposition goes further and gaseous oxygen (i.e., $^3O_2$ diradicals) is formed as a volatile product. Indeed, substantial degree of transfer of spin density from Ag(II) to O atoms in the metal's first coordination sphere is expected,[38] leading to ease of generation of oxo- free radicals. It may therefore be anticipated that solvated $Ag(HSO_4)_2$ in superacidic media will exhibit lack of thermodynamic stability and it will readily undergo redox reactions, just like other oxo- siblings of Ag(II) in the bulk. Moreover, it is supposed to oxidize species present in excess in the reaction environment, such as solvent molecules and in particular anions, since anions are always easier to oxidize than the corresponding neutral species.[39]

Following what we have learned from chemistry of Ag(II) with oxo- ligands, we would like to propose two tentative reaction equations corresponding to the chemical reaction step in the solvent of varying acidity

$$Ag(HSO_4)_{2(solv)} \rightarrow Ag^+ + HSO^-_{4(solv)} + HSO^\bullet_{4(solv)} \quad (\text{for } H_0 > -12) \tag{21}$$

$$Ag(HSO_4)_{2(solv)} + H_2SO_{4(solv)} \rightarrow Ag^+ + 2HSO^-_{4(solv)} + H_2SO^{+\bullet}_{4(solv)} \quad (\text{for } H_0 < -12) \tag{22}$$

These reactions lead to regeneration of Ag(I). The formation of $HSO^\bullet_{4(solv)}$ may be linked to the appearance of the additional cathodic wave in H_2SO_4 solutions (see Section 3.3); our surmise is that the free radical product of the chemical reaction is then reduced.

It is worth noticing that at standard conditions Ag(II) is not capable of oxidizing sulfate or hydrogensulfate anions to the corresponding free radicals; the E^0 value for the Ag(II)/Ag(I) pair is +1.98 V versus NHE,[1,2] quite similar to the corresponding value for the $S_2O_8^{2-}/2SO_4^{2-}$ two-electron couple (+2.01 V versus NHE);[40] yet the E^0 value for the $SO_4^{\bullet-}/SO_4^{2-}$ one-electron couple is independent of pH and it has been evaluated as ca. +2.6 V versus NHE.[26] But, as we have shown,[21] the $E^{o\prime}$ value for Ag(II)/Ag(I) in sulphuric acid is steeply dependent on the Hammett acidity function[30] and it reaches +2.9 V versus NHE in the superacidic conditions thus permitting Ag(II) to oxidize HSO_4^- anions via $1e^-$ process in the superacidic regime.

4. CONCLUSIONS

Results indicate that the silver(I) electrooxidation in concentrated sulphuric acid solutions and oleums proceeds according to E_qC_i' mechanism, that is the electron transfer is followed by a homogeneous chemical reaction. By means of digital simulations we have established that silver(I) is regenerated in the chemical step. Moreover, from comparison of experimental and simulated voltammetric courses we determined selected kinetic parameters of the electrode process. Activation energies of electrochemical and chemical step were similar $E_{A,E}$ = 52 kJ·mol^{-1} and $E_{A,C}$ = 60 kJ·mol^{-1}, respectively.

At higher Ag(I) concentrations, above 50 mM, it is possible to perform a batch electrolysis in 100% H_2SO_4 with the formation of dark yellow ESR-active solution which contains Ag(II) cations; a highly reactive dark brown powder slowly precipitates from these solutions. ESR spectroscopy and spectroelectrochemical measurements coupled with theoretical DFT calculations suggest that solvated $Ag(HSO_4)_2(H_2SO_4)_2$ or similar species are electrogenerated in 100% H_2SO_4. In these species, Ag(II) is found in a distorted octahedral (close to tetragonal) coordination with O atoms. Characterization of this solid will be reported in another contribution.

The formal potential of the Ag(II)/Ag(I) redox couple in 100% sulphuric acid is 2.6 V vs NHE;[21] furthermore, this value substantially increases with the increase of solution acidity. The formal potential reaches 2.90 V versus NHE in superacidic 30% oleum characterized by $H_0 = -14.0$. These results indicate that silver oxidation in superacidic media leads to the formation of particularly strong oxidizing, and relatively long-lived, species containing Ag(II).[41] The exceptionally powerful free-radical Ag(II) oxidizers could now be used for $1e^-$ oxidation of various kinetically inert systems (such as hydrocarbons) and in general for initialization of freeradical reactions in superacidic media.

■ ASSOCIATED CONTENT

Ⓢ Supporting Information

Additional information and figures. This material is available free of charge via the Internet at http://pubs.acs.org.

■ AUTHOR INFORMATION

Corresponding Author

*E-mail: rafjur@chem.uw.edu.pl. wgroch@chem.uw.edu.pl.

Notes

The authors declare no competing financial interest.

■ ACKNOWLEDGMENTS

This work has been financed by the National Science Centre (Poland) within the “OPUS” Programme (2011/01/B/ST5/06673). Access to the computer cluster halo2 operated by the Interdisciplinary Centre for Mathematical and Computational Modelling (ICM), University of Warsaw, has been granted within the project G29-3. Authors acknowledge Dr. J. Szydłowska for measuring of the ESR spectra. The study was carried out at the Biological and Chemical Research Centre, University of Warsaw. This work is dedicated to Professor Jacek Lipkowski of Guelph University, Canada.

■ REFERENCES

(1) Bard, A. J.; Parsons, R.; Jordan, J. *Standard Potentials in Aqueous Solution*; Marcel Dekker Inc: New York, 1985.

(2) Leszczyński, P. J.; Grochala, W. Strong Cationic Oxidizers: Thermal Decomposition, Electronic Structure and Magnetism of their Compounds. *Acta Chim. Slov.* **2013**, *60*, 455−470.

(3) Kumar, A. Kinetics of Oxidation of Ethanolamine and Diols by Ag (II). *J. Phys. Chem.* **1982**, *86*, 1674−1678.

(4) U.S. Patent 5,855,763, 1999.

(5) U.S. Patent 5,078,902, 1992.

(6) Boardman, D. W.; Lin-Cai, J.; Pletcher, D. The Catalysis of the Anodic Oxidation of Cobalt(II) and Manganese(II) by Silver(I) in Aqueous Sulphuric Acid. *J. Electroanal. Chem.* **1983**, *149*, 49−56.

(7) U.S. Patent 5,745,835, 1998.

(8) Bringmann, J.; Ebert, K.; Galla, U.; Schmieder, H. Electrochemical mediators for total oxidation of chlorinated hydrocarbons: formation kinetics of Ag(II), Co(III), and Ce(IV). *J. Appl. Electrochem.* **1995**, *25*, 846−851.

(9) Govindan, M.; Chung, S.−J.; Moon, I. −S. Simple Technical Approach for Perpetual Use of Electrogenerated Ag(II) at Semipilot Scale: Removal of NO and SO_2 as a Model System. *Ind. Eng. Chem. Res.* **2012**, *51*, 2697−2703.

(10) Pillai, K. C.; Chung, S. J.; Moon, I. -S. Studies on Electrochemical Recovery of Silver from Simulated Waste Water from Ag(II)/Ag(I) Based Mediated Electrochemical Oxidation Process. *Chemosphere* **2008**, *73*, 1505−1511.

(11) Mentasti, E.; Baiocchi, C.; Coe, J. S. Mechanistic aspects of Reactions involving Ag(II) as An Oxidant. *Coord. Chem. Rev.* **1984**, *54*, 131−157.

(12) Pourbaix, M. Atlas of Electrochemical Equilibria in Aqueous Solutions; NACE: 1974; p 644.

(13) Náray-Szabó, I.; Argay, G.; Szabó, P. The Structure of the Ag(I,III) Oxide Phases. *Acta Crystallogr.* **1965**, *19*, 180−184.

(14) Rance, P. J. W.; Nikitina, G. P.; Korolev, V. A.; Kirshin, Yu. M.; Listopadov, A. A.; Egorova, V. P. Features of Electrolysis of Nitric Acid Solutions of Silver I. Behavior of Ag(II) in HNO_3 Solutions. *Radiochemistry* **2003**, *45*, 346−352.

(15) Rechnitz, G. A.; Zamochnik, S. B. Spectrophotometric Investigation of the Nature and Stability of Silver(II) in Acidic Sulphate Media. *Talanta* **1964**, *11*, 1651−1655.

(16) Kodera, F.; Kuwahara, Y.; Nakazawa, A.; Umeda, M. Electrochemical Corrosion of Platinum Electrode in Concentrated Sulfuric Acid. *J. Power Sources* **2007**, *172*, 698−703.

(17) Pley, M.; Wickleder, M. S. $Pt_2(HSO_4)_2(SO_4)_2$, The First Binary Sulfate of Platinum. *Z. Anorg. Allg. Chem.* **2004**, *630*, 1036−1039.

(18) Arnaud, O.; Eysseric, C.; Savall, A. Optimizing the Anode Material for Electrogeneration of Silver(II). *Inst. Chem. Eng. Symp. Ser.* **1999**, *145*, 229−238.

(19) Racaud, Ch.; Savall, A.; Rondet, Ph.; Bertrand, N.; Groenen Serrano, K. New Electrodes for Silver(II) Electrogeneration: Comparison Between Ti/Pt, Nb/Pt, and Nb/BDD. *Chem. Eng. J.* **2012**, *211−212*, 53−59.

(20) Panizza, M.; Duo, I.; Michaud, P. -A.; Cerisola, G.; Comninellis, Ch. Electrochemical Generation of Silver (II) at Boron-Doped Diamond Electrodes. *Electrochem. Solid State Lett.* **2000**, *3*, 550−551.

(21) Połczyński, P.; Jurczakowski, R.; Grochala, W. Stabilization and Strong Oxidizing Properties of Ag(II) in a Fluorine-Free Solvent. *Chem. Commun.* **2013**, *49*, 7480−7482.

(22) Latinen, H. A.; Conley, J. M. Electrolytic Generation of Silver(II) at Antimony-Doped Tin Oxide Electrodes. *Anal. Chem.* **1976**, *48*, 1224−1228.

(23) Wardman, P. Reduction Potentials of one-Electron Couples involving Free Radicals in Aqueous Solution. *J. Phys. Chem. Ref. Data* **1989**, *18*, 1637−1755.

(24) Baxendale, J. H.; Fielden, E. M.; Keene, J. P.; Ebert, M. *In Pulse Radiolysis*; Keene, J. P., Swallow, A., Baxendale, J. H., Eds.; Academic Press: London, 1965, p 207.

(25) Eberson, L. *Electron Transfer Reactions in Organic Chemistry*; Springer-Verlag: Berlin, 1987.

(26) Liang, C.; Bruell, C. J.; Marley, M. C.; Sperry, K. L. Persulfate Oxidation for in Situ Remediation of TCE: I. Activated by Ferrous Ion with and without a Persulfate-Thiosulfate Redox Couple. *Chemosphere* **2004**, *55*, 1213−1223.

(27) Darling, H. E. Conductivity of Sulfuric Acid Solutions. *J. Chem. Eng. Data* **1964**, *9*, 421−426.

(28) Gillespie, R. J.; Robinson, E. A. Raman Spectra of the H_2SO_4−SO_3 and D_2SO_4−SO_3 Systems: Evidence for the Occurrence of Polysulphuric Acids. *Can. J. Chem.* **1962**, *40*, 658−674.

(29) Bard, A. J.; Faulkner, L. R. *Electrochemical Methods: Fundamentals and Applications*; Wiley: New York, 1980.

(30) Jorgenson, M. J.; Hartter, D. R. A Critical Re-Evaluation of the Hammett Acidity Function at Moderate and High Acid Concentrations of Sulfuric Acid. New H_0 Values Based Solely on a Set of Primary Aniline indicators. *J. Am. Chem. Soc.* **1963**, *85*, 878−883.

(31) Po, H. N.; Swinehar, J. H.; Allen, T. L. The Kinetics and Mechanism of the Oxidation of Water by Silver(II) in Concentrated Nitric Acid Solution. *Inorg. Chem.* **1968**, *7*, 244−249.

(32) Obviously, if the concentration of $HSO_4^{\bullet}$ radicals is large they might recombine into $H_2S_2O_8$ acid, which is likely undissociated in the presence of stronger H_2SO_4 or $H_2S_2O_7$ acids.

(33) Minner, E.; Lovy, D.; Bill, H. Electron Paramagnetic Resonance and Relaxation Study of Copper(II) and Silver(II) in $CsCdF_3$ Single Crystals. *J. Chem. Phys.* **1993**, *99*, 6378−6383.

(34) Malinowski, P. J.; Derzsi, M.; Gaweł, B.; Łasocha, W.; Jagličić, Z.; Mazej, Z.; Grochala, W. Ag(II)SO_4: a Genuine Sulfate of Divalent Silver with Anomalously Strong one-Dimensional Antiferromagnetic interactions. *Angew. Chem., Int. Ed.* **2010**, *49*, 1683−1686.

(35) Deno, N.; Taft, R., Jr Concentrated Sulfuric Acid-Water. *J. Am. Chem. Soc.* **1954**, *76*, 244−248.

(36) Malinowski, P. J.; Derzsi, M.; Mazej, Z.; Jagličić, Z.; Leszczyński, P. J.; Michałowski, T.; Grochala, W. Silver(II) Fluorosulfate: a thermally Fragile Ferromagnetic Derivative of Divalent Silver in An Oxa-Ligand Environment. *Eur. J. Inorg. Chem.* **2011**, 2499−2507.

(37) Malinowski, P. J.; Mazej, Z.; Derzsi, M.; Jagličić, Z.; Szydłowska, J.; Gilewski, T.; Grochala, W. Silver(II) Triflate with one-Dimensional $[Ag(II)(SO_3CF_3)_{4/2}]_\infty$ Chains Hosting Antiferromagnetism. *Cryst. Eng. Commun.* **2011**, *13*, 6871−6879.

(38) Grochala, W. Beyond Fluorides: Extension of Chemistry of Divalent Silver To Oxo Ligands. *Inorg. Chem. Commun.* **2008**, *11*, 155−158.

(39) For diluted H_2SO_4 solutions, water is likely to be oxidized.

(40) Vanýsek, P. Electrochemical Series. In *Handbook of Chemistry and Physics*, 93rd ed; Haynes, W. M., Ed.; CRC: Boca Raton, FL, 2012; pp 5−80.

(41) Our results indicate that Ag(I)HSO_4 dissolved in the concentrated sulphuric acid is not oxidized by ozone (5% O_3, 95% O_2, no moisture) even after prolonged treatment up to 48 h.

(42) Dogliotti, L.; Hayon, E. Flash Photolysis of Persulfate Ions in Aqueous Solutions. Study of the Sulfate and Ozonide Radical Ions. *J. Phys. Chem.* **1967**, *71*, 2511−2516.